ISTITUTO NAZIONALE DI FISICA NUCLEARE

Sezione di Milano

INFN/TC-91/10
7 Novembre 1991

L. Rossi, G. Volpini:

A NEW SCHEME FOR CRITICAL CURRENT MEASUREMENTS ON STRAIGHT SUPERCONDUCTING CABLES IN A LARGE SOLENOID

Servizio Documentazione
dei Laboratori Nazionali di Frascati

A new scheme for critical current measurements on straight superconducting cables in a large solenoid

L. Rossi and G. Volpini

Dipartimento di Fisica dell' Università di Milano
and
Istituto Nazionale di Fisica Nucleare sezione di Milano
LASA Laboratory
via F.lli Cervi, 201 20090 SEGRATE (MI) I

October 24, 1991

Abstract

The precision of I_C measurement of straight superconducting cables in solenoids can be limited by the magnetic field inhomogeneity. A solution in order to improve the field homogeneity based on iron shims is presented here. A conceptual design for the experimental lay–out of a test station to be used in connection with the SOLEMI–I solenoid at the Milan INFN Section (LASA Laboratory) is given.

1 Introduction

The new accelerator for high-energy physics foreseen at CERN, the LHC (Large Hadron Collider), requires the construction of some 1,600 superconducting *two–in–one* dipoles 10–m long with a nominal field of 10 Tesla, along with many other focusing quadrupoles, sextupoles, correcting dipoles, etc. This large scale production of SC magnets will require approximately 4,000 km of SC cable with high performances ($J_C \simeq 1,300\ A/mm^2$ at 4.2 K, 8 T; $\phi_{filaments} \simeq 5\mu$), which is under development by several European industries.

In order to test the performances of these cables and to investigate their physical properties a new test station is at present under construction in Milan [1],[2]. The work on the I_C measurements has produced in the last years a large effort both for the definition of critical currents [3],[4],[5] and for the experimental arrangement [6]. Purpose of this work is to present a new experimental solution devised for Milan's test station.

2 Current measurement systems

Superconductivity can only exist when temperature, magnetic field and transport currents are below some values, characteristic of each material. If we plot these values on a J, T, B graph, we obtain the so–called *critical surface.*

In order to perform correctly the measurements, all the relevant physical quantities must be well-defined. While no problem arises with transport current flowing in the sample, that can be known with an accuracy of $10^{-3} \div 10^{-4}$, and with temperature, that can be measured within $\sim \pm 0.01$ K in equilibrium conditions, the magnetic field has often an ill–defined value due to its inhomogeneity in the measuring zone, and this reflects on the accuracy by which the I_C can be measured. Other factors can worsen the accuracy of I_C measurements, like the pressure on cable that arises because of the interaction between current flowing in the cable with the total magnetic field, and the lack of cable cooling that may cause premature quenching. In cables with high I_C, like those of LHC dipoles, the situation is even worse, since in this case we have to face a large self–field effect;

the current distribution among the different strands is not known *a priori* and this introduces a further source of uncertainty. In any case in defining the field inhomogeneity we explicitly do not take into account the self–field coming from the current flowing in the sample itself, being our analysis concerned on the applied field.

In the so–called *hairpin* geometry a wire is simply bent in a U–shape, with the voltage taps put across the short horizontal zone. Usually the sample holder is inserted into a small solenoid in such a way that the horizontal measuring zone is perpendicular to the solenoid field. In this case the sample is very short and usually experiences a field inhomogeneity of the order of 5 – 10 %. In order to increase the useful length, and thus the sensitivity, the wire can be wound onto a small cylinder. Moreover in such a system the applied field on the sample is uniform. This last system is the most diffuse for I_C measurements of wires and small cables.

More problems appear when cables with several thousands Amps of I_C are considered, like those for accelerator dipoles. They have a trapezoidal section, with an high aspect ratio (the ratio between the width and the thickness of) and a small keystone angle (the angle between the two broad faces). I_C must be measured with the applied field perpendicular to the broad face. Use of a solenoid to provide the background field suggests to bend the cable in a loop in order to take advantage of the magnet symmetry both for the field homogeneity and for the forces exerted onto the sample. Unfortunately bending of the cable on a relatively small diameter (200–400 mm) with respect to the cable width ($\sim$ 20 mm) results in a severe influence on the I_C, mainly because of stresses and current redistribution among the strands. For such a cable the most straightforward system for I_C measurements is to use the free bore of a dipole, where the cable can be arranged in straight lengths, like the BNL facility, at present the world leader for such a measurement [7]. Another solution in order to have a better external field is based on a split–coils geometry [8]. These two solutions have the disadvantage that both require an ad–hoc device, often more expensive than a general–purpose solenoid.

Despite the above–mentioned difficulties I_C measurements can be done in a solenoid with the sample arranged in a loop. At Genoa University such a facility has worked with a 6 T solenoid ($\phi_{loop} \sim 400$ mm) and it is being upgraded to 8 T ($\phi_{loop} = 250$ mm) using an inductive method to supply a

transport current up to 60 kA [6].

We propose an experimental layout with the cable is simply bent in a U–shape, with the short horizontal segment perpendicular to the field, and in which the applied field in the measuring zone is made homogeneous by means of fully saturated iron shims. We prove in the next part that this solution is practically feasible, and that it allows to have a field homogeneity, defined as $(B_{max} - B_{min})/B_0$ in the relevant region of about 0.5%, for a solenoid field from 6 to 8 Tesla.

3 Iron shim design

3.1 The physical statement of the problem

The iron shim design can be mathematically described as follows: the flux density $\vec{B}$ produced by a current $\vec{J}$ is given by the Ampère law:

$$\nabla \times \vec{B} = \mu_0 \vec{J} \tag{1}$$

whose most general solution is:

$$\vec{B}(\vec{x}) = \nabla \times \frac{\mu_0}{4\pi} \int \frac{\vec{J}(\vec{x}')}{\mid \vec{x}' - \vec{x} \mid} d^3x'. \tag{2}$$

In the case of an air coil solenoid made out of round current loops eq. 2 may be solved in terms of elliptical integrals. Since the field is not homogeneous inside the solenoid, we want to introduce some ferromagnetic material in order to correct the field in a given space region. Eq. 1 can be generalized to the case in which we have both magnetic materials and currents:

$$\nabla \times (\frac{\vec{B}}{\mu_0} - \vec{M}) = \vec{J} \tag{3}$$

where $\vec{M}$ is the magnetization. This is quite a complicated equation for ferromagnetic material since $\vec{M}$ is a non–linear function of $\vec{H}$. In our case, with a solenoid field of 6 T or greater, we can assume that the iron is fully saturated, $\vec{M}$ then reduces to a constant with $\mid M \mid \simeq 2.1$ T. Because of the finite length of the solenoid the field lines are not parallel to the z–axis, furthermore the iron shims have not a null demagnetization factor;

as a consequence the magnetization can not be uniform. In any case we point out that in the region of interest, about 20 mm far from the median plane, the field is almost parallel to z, within 0.5 degree, and it is so large that the contribution of the demagnetization effect is completely negligible, so that it can safely be assumed $\vec{M} \parallel \vec{B}_C \parallel z$, where $\vec{B}_C$ is the magnetic field provided by the air core solenoid. The total field inside solenoid is $\vec{B} = \vec{B}_C + \vec{\tilde{B}}$, where $\vec{\tilde{B}}$ is the contribution from the shims. $\vec{B}_C$ is provided by equation eq. 2, (where J is now the transport current flowing inside the solenoid), and $\vec{\tilde{B}}$ is

$$\vec{\tilde{B}} = \nabla \times \frac{\mu_0}{4\pi} \int \frac{\nabla \times \vec{M}}{\mid \vec{x} - \vec{x}' \mid} d^3x. \tag{4}$$

Since the value of $\vec{M}$ is uniform in the iron, the above integral reduces to an integral over the volume surface, where the term $\nabla \times \vec{M}$ is equivalent to surface magnetization current $\vec{J}_{SM}$.

From an intuitive point of view we assume that in order to have a uniform field on the median plane we need two iron shims, placed symmetrically respect to the median plane. It is expected that these shims will be thicker in the central region (where the solenoid field is weaker) and thinner in the outer region, the shape being described by two curved surfaces. From a mechanical point a view, a stepwise surface is much more easily machined than a arbitrary curved surface (see fig.1).

For such a shape the iron shims are equivalent to a set of solenoids placed on the cylindric surfaces of the shim, with a surface current density given by the saturated value of magnetization, $J_{SM} = M_{sat}$; in this case the total field (field from solenoid plus field from iron) can be expressed in terms of elliptical integrals. Once the shim geometry is known, the field can be easily calculated. In sec. 3.3 we solve the inverse problem, that is to find the dimensions of the shim from the desired shape of the field. This process will be called *shim optimization.*

It is apparent from the above considerations that an ideal optimization, i.e. one for which the field on the median plane is exactly constant, may be obtained at most for one given value of the solenoid central field. If the same shims are operated with a different solenoid central field, the total field in the median plane is no longer constant. Before calculating explicitly the

shape of the iron shim now we want to answer to the following question: if we want to operate between two values of solenoid central field, say B_1 and B_2, at which value should be performed the optimization, and what is the worst homogeneity obtained when the solenoid central field is swept between B_1 and B_2 ?

3.2 On the maximum attainable correction

Let's assume that for a value B_0 of the solenoid central field we have a perfect optimization, that is the total field on all the points of median plane is equal to $B_C(0,r)+\tilde{B}(0,r) = cost$, where $\tilde{B}(0,r)$ is the contribution coming from the iron shims.

The solenoid field on the median plane may be expressed in terms [9] of a power expansion of the form:

$$B_C(0,r) = B_0 \cdot (1 + \sum_k A_k r^k), \qquad k = 2,4,\ldots \tag{5}$$

a perfect correction for a given value of B_0 may then be reached if the contribution from the iron shims looks like

$$\tilde{B}(0,r) = \tilde{B}_0 - B_0 \sum_k A_k r^k, \qquad k = 2,4,\ldots \tag{6}$$

where $\tilde{B}_0$ is the contribution of the iron to the central field.

It is clear that for any other value of the solenoid central field the optimization is no longer perfect, since the solenoid field at any point r scales linearly with the central field, whilst the correction field remains constant, at least as long as the iron contribution may be regarded as constant. It is interesting to find out what is the best homogeneity achievable on a given range of solenoid central field B_1–B_2, as a function of B_0, the field at which the optimization has been performed.

The maximum absolute inhomogeneity for an arbitrary solenoid central field B' is defined as

$$\begin{aligned} \Delta B = B_{max} - B_{min} &= |B_{edge} - B_{center}| \qquad (7) \\ = |(B' + B' \sum_k A_k R^k + \tilde{B}_0 - B_0 \sum_k A_k R^k) - (B' + \tilde{B}_0)| & \\ = \sum_k A_k R^k \cdot \mid B' - B_0 \mid, & \end{aligned}$$

where R is the maximum value of r at which optimization is performed. The relative inhomogeneity is then:

$$\frac{\Delta B}{B_{center}} = \sum_k A_k R^k \cdot \frac{|B_0 - B'|}{B' + \tilde{B}_0}. \tag{8}$$

The inhomogeneity is therefore 0 for $B' = B_0$, for $B' \neq B_0$ increases linearly; it reaches its highest value when $B' = B_1$ or $B' = B_2$. Now let's consider B_0 as a running parameter, in fig. 2 it is reported the relative inhomogeneity at the two values B_1 and B_2 as a function of B_0. The full line represents the worst value over the range B_1–B_2. It is apparent that best homogeneity is reached at that value of B_0 where the two straight lines cross; and from simple algebra this value is found to be

$$B_0 = \frac{\tilde{B}_0(B_1 + B_2) + 2B_1B_2}{2\tilde{B}_0 + B_1 + B_2}. \tag{9}$$

In our case B_1= 6T, B_2= 8T and $\tilde{B}_0 \sim 0.25$ T. The best value at which optimization should be performed is then found from eq. 9 to be 6.86 T. This value is almost independent of $\tilde{B}_0$, since $\tilde{B}_0 \ll B_1, B_2$ and therefore terms in which $\tilde{B}_0$ appears are small; in practice the result does not change for any value of $\tilde{B}_0$ from 0.15 to 0.5 T. The maximum homogeneity achievable is calculated from eq. 8 to be 0.52 %. To solve this, we need not know the detailed value of $\{A_k\}$, but only the sum $\sum_k A_k R^k$ that in our case turns out to be 3.8% for R=21 cm.

3.3 The mathematical description

In order to solve practically the above problem, the optimization on the median plane will be performed on a given mesh, described by a set of m radial points $\{r_1, r_2, \ldots, r_m\}$. The optimization is made starting from a first feasible design and then changing the geometrical dimensions until a better solution is obtained. A dedicated computer code for this task is explained in this section. At present only the height of each iron disk can be varied, while the radii are kept fixed. This has been done for seek of simplicity; a improved version of the program that allows to change all the geometrical parameters is foreseen.

From a mathematical point of view, the optimization process described above amounts to minimize the function

$$\sum_{i=1}^{m}(B_{r_i} - B)^2, \tag{10}$$

where B_{r_i} is the field at the point r_i, and B is the optimized field value pursued.

The two iron shims are identical and can be described by means of $2n+1$ parameters $s_i, t_i, c \quad i = 1, \ldots, n$ where n is the number of iron disks, s_i and t_i are the height and the radius of the lower edge of each disk (see fig. 1), and c is the upper plate height.

The geometrical parameters being varied are bound to some constraints (the height of each disk can not be less than zero):

$$s_j \leq s_{j+1} \qquad j = 1, 2, \ldots, n \qquad s_{n+1} = c \tag{11}$$

In principle other constraints could be added, e.g. imposing that the total height of the shim be equal to a given value, as well as other values now being kept fixed (like the final field value B in eq. 10) could come into play. This requires only minor modifications to our program, and it will likely be done in the future.

Now let's write down explicitly eq. 10. First suppose we have a first feasible solution, described by a set of values

$$s_i^{(0)} \; t_i^{(0)} \; c^{(0)}, \qquad i = 1, 2, \ldots, n. \tag{12}$$

The total field at point r_i, B_{r_i}, is the sum of the solenoid field, $B_{r_i}^{ext}$, plus the field produced by the iron shims. From what has been discussed in sec. 3.1 it is clear that the iron shims may be approximated as a set of solenoid with radius t_i and height $s_{i+1} - s_i$, and with surface current density $J_{SM} = M_{sat}$; then B_{r_i} looks like:

$$B_{r_i} = B_{r_i}^{ext} + \sum_{j=1}^{n} f(s_j, s_{j+1}, t_j, r_i), \tag{13}$$

where $f(s_j, s_{j+1}, t_j, r_i)$ is the contribution to field at point r_i coming from the $j - th$ disk. Now we can express this factor form f as a power

expansion in terms of $h_j = s_j - s_j^{(0)}$. Taking terms up to the first order and substituting in eq. 10 we obtain

$$\sum_{i=1}^{m}\Big(B_{r_i}^{ext} - B + \sum_{j=1}^{n} f(s_j^{(0)}, s_{j+1}^{(0)}, t_j^{(0)}, r_i) + \sum_{j=1}^{n} \frac{\partial f(s_j, s_{j+1}, t_j^{(0)}, r_i)}{\partial s_j}\Big|_{s_j = s_j^{(0)}}^{s_{j+1} = s_{j+1}^{(0)}} \cdot h_j\Big)^2, \tag{14}$$

that can be rewritten, with obvious notation, as:

$$\sum_i (a_i + \sum_j b_{ij} h_j)^2 \;=\; \sum_i a_i^2 + 2\sum_{ij} a_i b_{ij} h_j + \sum_j \Big(\sum_s h_s b_{sj}\Big)\Big(\sum_i b_{ji} h_i\Big). \tag{15}$$

Eq. 15 can be rewritten in matrix notation, with $\underline{A} = \{a_i\}$, $\underline{H} = \{h_i\}$ and $\underline{\underline{B}} = \{b_{ij}\}$. The first term, $\sum_i a_i^2$, can be neglected since it is constant and therefore has no influence in the minimization process.

$$(\underline{A}^T \underline{\underline{B}})\underline{H} + \frac{1}{2}\underline{H}^T(\underline{\underline{B}}^T \underline{\underline{B}})\underline{H}. \tag{16}$$

Constraints (11) are now rewritten as

$$h_j \geq -(s_{j+1}^{(0)} - s_j^{(0)}) \tag{17}$$

The problem expressed by eq. 15 or 16, along with constraints (17) is well–known in the optimization theory with the name of *quadratic programming*, and the function to be minimized is referred as *objective function.* In the next section this problem will be explicitly solved. Now we want to emphasize that eq. 15 or 16 are only a first–order approximation of eq. 10, and it is therefore of great importance to start from a first feasible solution (12), already known to be a good approximation, in order to have a fast convergence of the solution.

3.4 The implementation of the alghoritm and the results

The computer code exploits the routine E04NAF taken from NAG library, which is devoted to the solution of quadratic programming problems. Starting from a given first feasible solution, the program gives the suggested

changes of the iron disk heights. The effect of these changes is then evaluated explicitly by means of another computer code which can calculate with (in principle) an arbitrary precision the magnetic field produced by the system solenoid plus iron shims. The new solution along with its field map on the median plane can be reintroduced in the optimization program in order to have an improved accuracy.

No cross–check of optimization program is needed, since the exact effect of the new design is explicitly verified. In fig. 3 the result of two iterations is shown. The full line is the total field on the median plane with an 'hand–made' design of the iron shim; stars and dots represent, respectively, two subsequent iterations. It is seen that a good result is rapidly achieved.

In fig. 4 median plane field is shown for an iron shim optimized for a 6.86 T solenoid central field. Squares refer to the field with a solenoid field of 6.86 T (the optimization value), dots to the case with a solenoid field of 6 T and stars to the case with 8 T. Field values on the y–axis are expressed as differences from the central field value for each case, in order to compare them. In the three cases following homogeneity is achieved:

B_{max}	B_{min}	ΔB	B_{center}	inhomogeneity
8.2914	8.2461	0.0453	8.29	0.55 %
7.1016	7.0965	0.0051	7.10	0.07 %
6.2389	6.2073	0.0316	6.24	0.51 %

As can be seen, results are in good agreement with the estimate of eq. 8. We regard this value of inhomogeneity as acceptable, since the field homogeneity is spoiled also by the cable self-field, which can be as high as 0.5 T It must be emphasized, however, that those two inhomogeneities (i.e. self-field and solenoid field inhomogeneity) do not compare, since the former is experienced only by a part of the cable, while the latter is homogeneous on a full section. Nonetheless this points out that a great effort in order to get an applied field homogeneity better than 0.5% is not worth.

4 The general lay–out of the measuring station

The iron shims are the new feature of our apparatus. Now we pass to describe briefly the other details. A preliminary design is shown in fig. 5. The sample is composed by two sections of cable, soldered at one end, while at the other end they are connected to the current leads. In order to accommodate the cable and to keep tight the whole system, stainless steel plates are put between the sample and the iron shims, as well as outside the iron shims. The whole system of sample, iron shims and stainless steel plates is kept fixed by means of screws.

4.1 Forces on the cable

A major problem in our scheme are the electromagnetic forces exerted on the sample cable. A straight cable, carrying 30 kA in a 8–T applied field experiences a net force of 240 kN$\cdot m^{-1}$, i.e. some 100 kN in our case. A widely used solution is to have two cables, electrically insulated but tightly clamped together, carrying the same current flowing in opposite directions. In this way no net external force remains, but for the unbalanced section of cable between current leads. This leads, depending on the exact path of cables, either to a residual lateral net force of 20 kN, or to a torque of $\sim$ 1kN$\cdot$m; in both case forces or torques should be supported by the helium vessel.

We are investigating a solution where forces are discharged directly onto the cryostat bottom plate to avoid excessive stress on the weldings. This bottom plate is kept in position by means of a set of pretensioned titanium rods so that forces are eventually discharged on the bottom plate of the vacuum chamber, at 300 K.

In our design the internal repulsive force should be borne by twelve screws. In order to accommodate the screws, twelve holes should be done in each iron shim. The effect of these holes, with a diameter of 10 mm, is about 0.03 % of the field at 6 T, and as such it can be neglected.

4.2 Current leads

Special design current leads from Fuji (J) have been adopted. They are optimized for a steady current of 12,000 A and they can withstand 30,000 A for a period up to 3 minutes with only boil–off helium cooling. Better performance can be obtained with helium extra–cooling. Consumptions for each current lead are reported in the following table.

I (kA)	$\dot{Q}$ (Watt)
0–8	~ 10
12	~ 14
22	~ 26
30	~ 42

A description of a possible measurement cycle is given in the next table, along with the estimated consumption for each lead. The total helium consumption is expected to be $\sim$ 40 litres.

time	current (kA)	power (W)	consumption (liters of helium)
30'	fill–up	10	7
10'	< 8	10	2.5
10'	< 12	14	3.5
5'	< 22	26	3
5'	< 30	42	5

The measurement time lenghts quoted are estimated in order to allow the current to distribute uniformly among strands.

4.3 Cryostat design

In this section we make an estimate of the cryostat consumption. Since we found that this is largely smaller than the consumption for a measuring cycle, no special effort has been done in order to optimize the cryostat from this point of view.

4.3.1 Liquid helium consumption estimate

The losses for thermal conduction in the helium cryostat, radiation from the nitrogen shield and funneling are estimated as follows:

- Thermal conduction between helium temperature and liquid nitrogen temperature for a 5–mm thick 50–cm wide helium can, where the helium level is 40 cm far from the liquid nitrogen point, is:

$$P(Watts) = \frac{A}{L} \cdot \int_{4\ K}^{77\ K} \lambda dT = \frac{79(cm^2)}{40(cm)} \cdot 3(Watt \cdot cm^{-1}) = 5.9 \quad (18)$$

  If no LN_2 (or gas cooled) shield were present, heat flowing directly from room temperature to helium bath would be at least twice as high for any reasonable geometry of cryostat.

- Radiation losses from the LN_2 shield to helium cryostat.
  Covering the LN_2 shield with commercial isolating aluminum tape can be reduce the emittance down to 30 mW/m^2 without special care for surface conditions. In this case the total heat flux from nitrogen to helium turns out to be $\sim$ 100 mW, that would rise up to $\sim$ 280 mW for a nitrogen shield temperature of $\sim$ 100 K. This contribution is therefore negligible if compared to the heat conduction in the cryostat wall. Also in this case, should no thermal radiation shield be present, the radiation flux from room temperature to liquid helium vessel would be $\sim$ 23 Watts.

- Funneling
  Radiation flowing from top of cryostat (at room temperature) to liquid helium is expected to be less than 5 Watts, and it can be reduced of one order of magnitude by means of a few shielding disks.

Summing up the three above contributions, the total heat flow in helium is expected to be < 7 Watts, coming chiefly from heat conduction. This value amounts to 10 liters of liquid helium boil–off per hour. It is worth pointing out that this is a preliminary and conservative estimate, and that a better design of the cryostat could reduce significantly liquid helium consumption. If superfluid helium is to be used a λ–plate is foreseen with a cooling power of 5 Watts at 2.2 K. The bus–bars used to feed the sample through the λ–plate should consume about $\frac{1}{2}$ liter of liquid helium per hour.

4.3.2 Liquid nitrogen consumption estimate

Calculations for heat flux on the nitrogen shield are analogous to those for helium.

- Thermal conduction between nitrogen and room temperature
  In this case the integrated conductivity is 27 $Watts \cdot cm^{-1}$, and the total heat flux is $\sim$ 100 Watts for a 5 mm thick wall and a distance of 20 cm between room temperature point and liquid nitrogen shield.

- Radiation flux form outer vessel to nitrogen shield
  Liquid nitrogen shield may be isolated from the outer vessel by means of either highly reflecting surfaces or multiple aluminized mylar layers (superinsulation). In both cases the heat flux lies in the range of 10–20 Watts.

Even in this case the larger contribution of heat flux comes from thermal conduction. The total heat flux is $\sim$ 120 Watts or $\sim$ 3 l/h of liquid nitrogen.

Since the radiation shield is kept at liquid nitrogen temperature only on a loop, the largest part of the shield is cooled via thermal conduction. In order to have a correct transfer of heat inside the radiation shield, its thickness must be thoroughly evaluated. This should be large enough not to have an exceedingly large temperature gradient inside the shield. If the maximum ΔT must be less than 10 K, shield thickness should be at least 2.2 mm (for a copper shield) or 3.6 mm (for an aluminium shield).

Another solution is to join the radiation shield to a suitable point of the helium cryostat neck. In this case the shield is cooled by the helium gas evaporated from the bath. This solution is mechanically simpler and easier to operate, on the other hand helium consumption is increased of about 30% compared to the liquid nitrogen cooled radiation shield. In both cases vertical cuts should be made on the shield in order not to have too large eddy currents.

5 Conclusions and Acknowledgments

We have presented a conceptual design for a device to measure I_C for straight cables. Whilst the magnetic parts (i.e. the iron shims) are near to a

final definition, mechanical design is only preliminary and further work is required before constructing. Following items should be investigated, among the others; residual forces and torques between dipole and iron shims, due to their misalignment, or between the current leads and the solenoid.

The authors wish to acknowledge prof. E. Acerbi for the fruitful discussions that led to the idea of a field corrector based on iron shims.

References

[1] E.Acerbi *et al.*, "Progress report of the high field superconducting facility at LASA laboratory", presented at the 11th International Conference on Magnet technology, August–September 1989, Tsukuba, Japan

[2] E.Acerbi *et al.* "The 18 Tesla 100 mm 4.2 K Free Bore Solenoid for LASA, Milan", presented at the at the 12th International Conference on Magnet technology, June 1991, Leningrad, USSR

[3] P.Fabbricatore *et al.* "Self field effects in the critical current measurements of superconducting wires and cables", Cryogenics **29,** Sept. 1989

[4] P.Fabbricatore *et al.* "Field inhomogeneity effects on the relation between short sample critical current and the quench current of high field dipole magnets", presented at the 11th International Conference on Magnet technology, August–September 1989, Tsukuba, Japan

[5] P.Fabbricatore *et al.* "Calculation of the effective critical field of the cable for the LHC dipole magnets", INFN/TC–90/08, 27 aprile 1990.

[6] P.Fabbricatore *et al.* "Critical Current of Prototype Conductors for the LHC dipole magnets", IEEE Transactions on magnetics, **MAG–27,** vol. 2, March 1991

[7] M. Garber and W. B. Sampson "Critical Current Measurements of Isabelle Superconducting Cables". BNL Technical Note No. 349, January 26, 1982.

W.B.Sampson, "Procedures for measuring the electrical properties of superconductors for accelerator magnets", ICFA Proceedings of Workshop on Superconducting Magnets and Cryogenics. Brookhaven National Laboratory, BNL 52006, May 12–16 1986, pagg. 153–156.

[8] H.H.J. ten Kate *et al.*, "A Test Facility for High–Current Superconducting Cables up to 25 kA at 7 Tesla", presented at the 11th International Cryogenic Engineering Conference (ICEC), Berlin, West–Germany, April 22–25 1986.

[9] Martin N.Wilson, *Superconducting Magnets*, pag. 26, Clarendon Press, Oxford 1983.

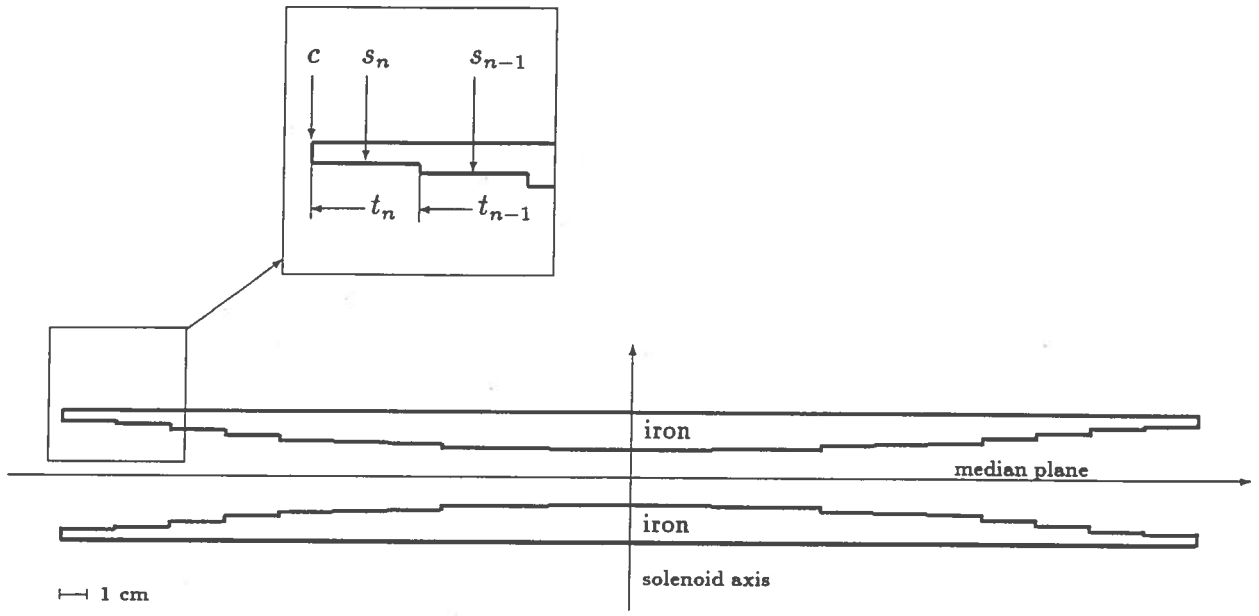

Figure 1: Iron shim design. The two shims have a cylindrical symmetry around the solenoid axis, as well as a reflexion symmetry around the median plane. In the enlarged box are reported the definitions for shim dimensions.

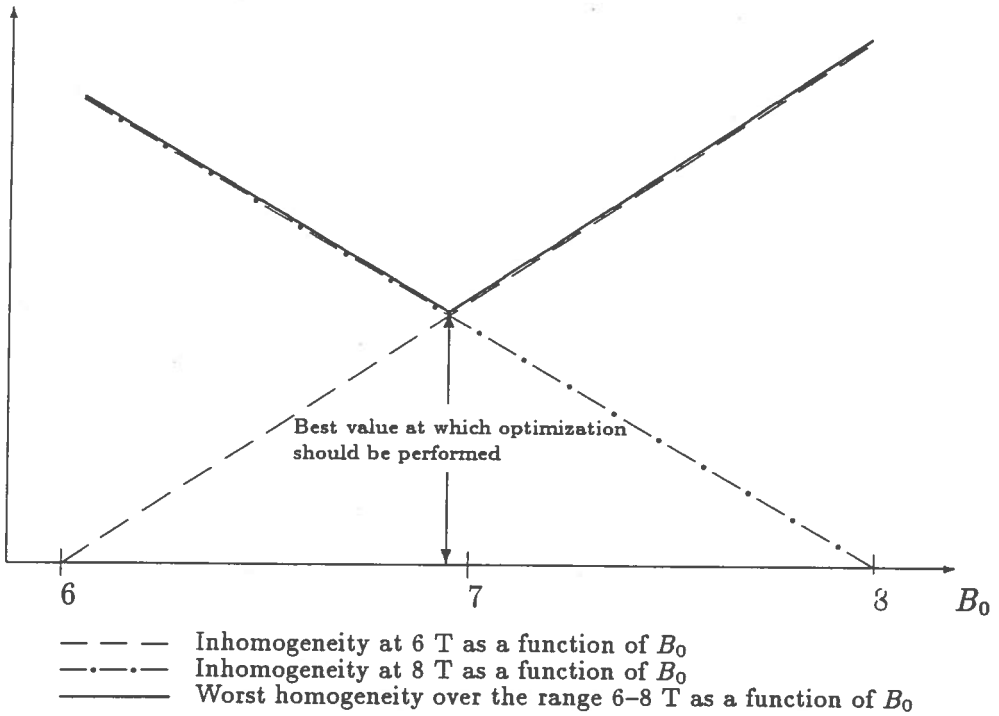

Figure 2: Maximum field inhomogeneity over the range 6–8 Tesla, as a function of B_0, the field at which optimization is performed.

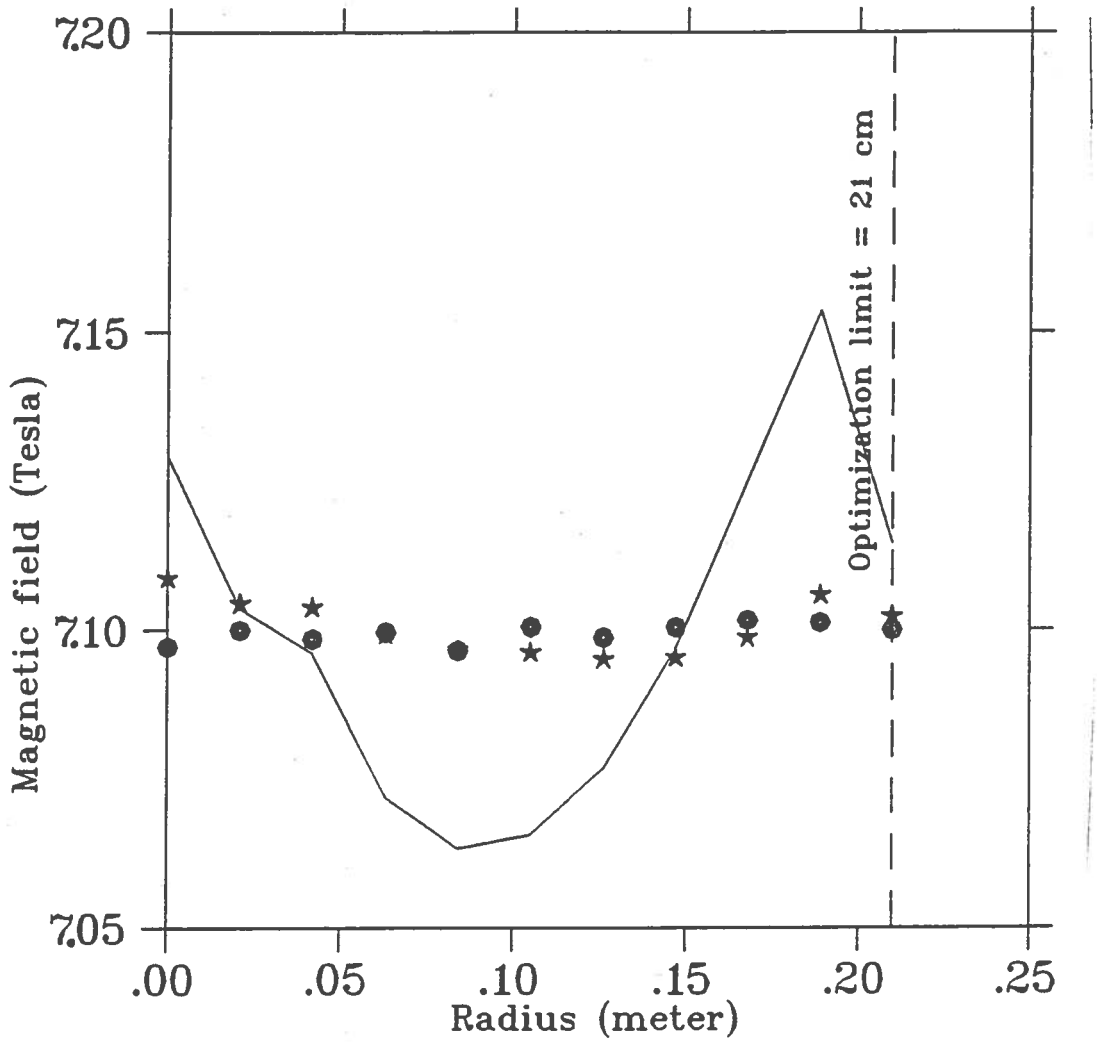

Figure 3: Field distribution on the median plane at different steps of optimization process: full line represents an 'hand–made' shim design, stars and dots refer to two optimization iterations. It can be seen that a good result is rapidly achieved.

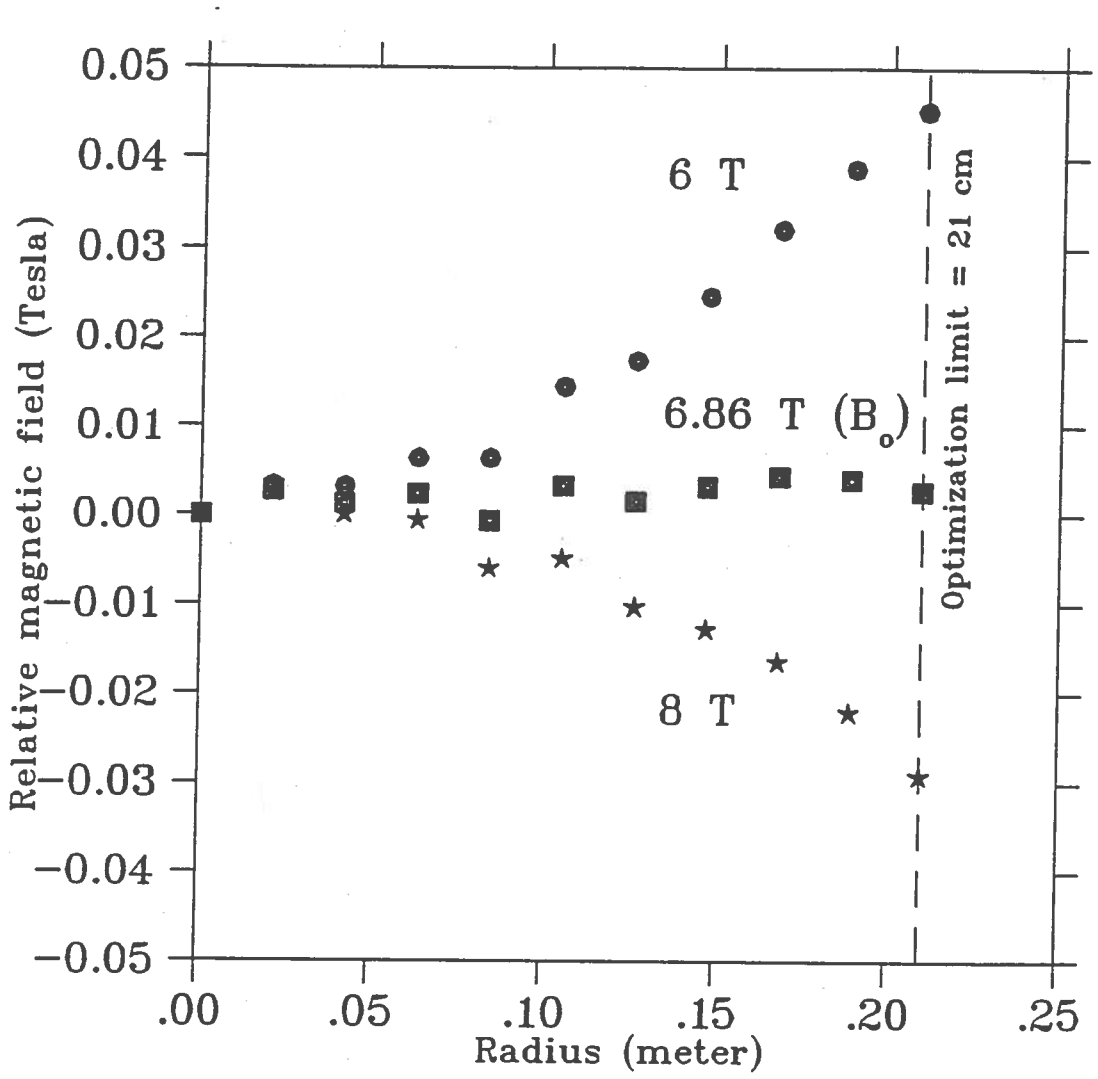

Figure 4: Median plane field at 6, 6.86 and 8 T for a shim optimized at 6.86 T, for a radius of 0–21 cm. Field values on the y–axis are expressed as differences from the central field value for each case, in order to compare them.

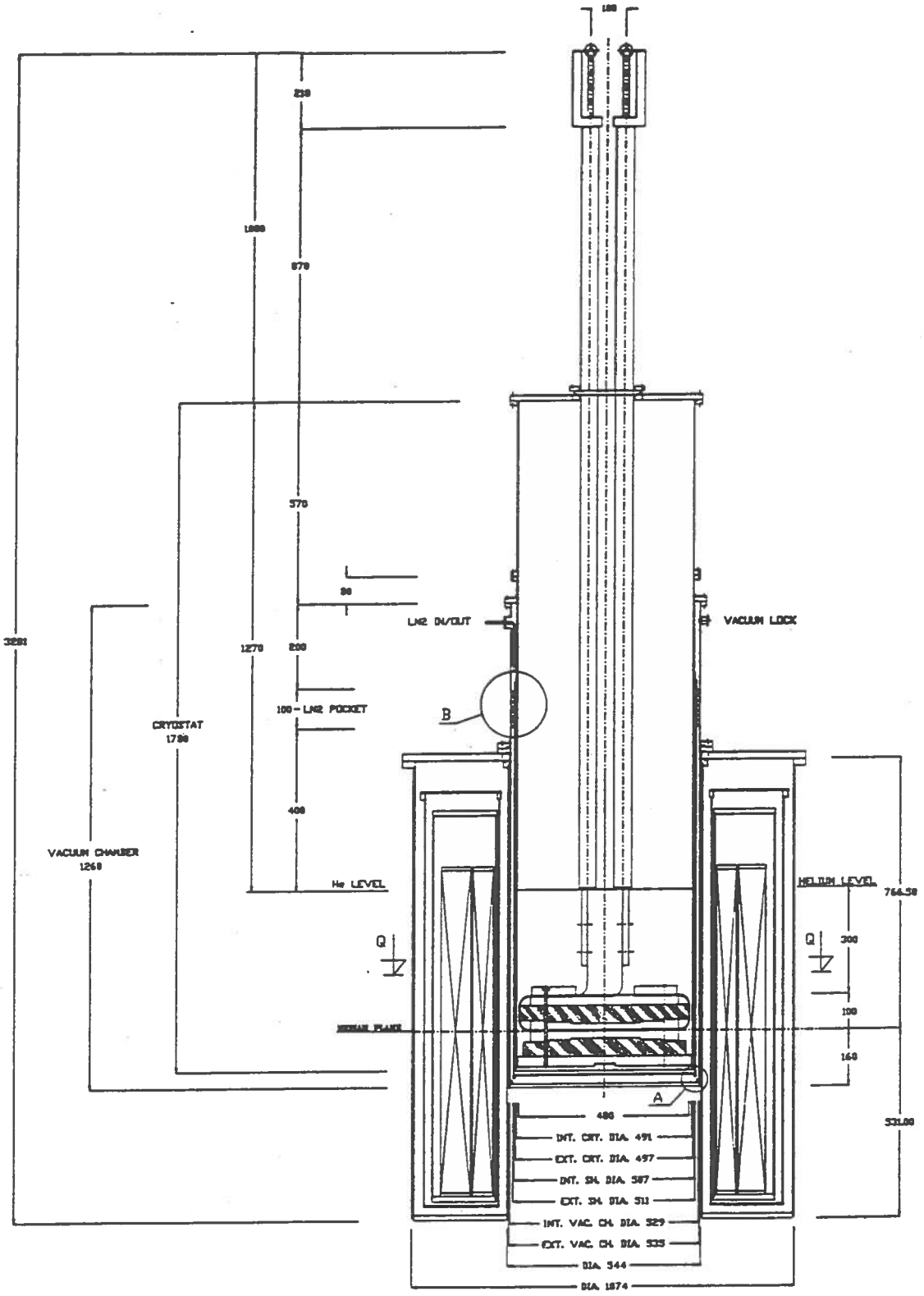

Figure 5: General lay–out of the measuring apparatus inside the SOLEMI-I apparatus. Iron shims are dashed.

Contents